# Testing the Sensitivity of a Neural Based Identification Algorithm to Shielding Levels

P. L. Lagari, S. Weidenbenner, M. Alamaniotis, C. K. Choi, L. H. Tsoukalas

*Nuclear Engineering Purdue University, 400 Central Dr., W. Lafayette, IN, 47907*
*{plagari, sweidenb, malamani, choi, tsoukala}@ecn.purdue.edu*

## INTRODUCTION

Radionuclide identification is an issue of great importance, especially nowadays for nuclear security [1], [2]. The nonproliferation of the Special Nuclear Materials (SNM) program emphasizes the above claim. Ports, airports as well as ground entry points in the US should be guarded and controlled so that hazardous materials, such as SNM, would not go through. To block these materials, the first step is to identify them among others, with a non-destructive and quick procedure, in order to avoid serious delay issues.

The present article aims to investigate the influence of building materials shielding, on the identification of a radioactive source by its gamma-ray spectrum. This is especially important for the detection of concealed radioactive sources and contributes to the national effort for nonproliferation and nuclear security. The conclusions may also be useful as far as shielding for radiation protection is concerned.

Here we consider passive detection, i.e. no external excitation is used as for example in Nuclear Resonance Fluorescence methods, where an external photon beam is used to trigger nuclear excitation and subsequent de-excitation.

The approach we followed has two main steps. At first we used the "GAmma Detector Response and Analysis Software" (GADRAS), developed at Sandia National Laboratory, [3] to simulate common practical shielding materials with various thicknesses. We have considered shielding thicknesses and materials to reflect buildings found in the Purdue University campus in West Lafayette, IN. Based on the campus structures, we selected three different shielding materials: concrete, wood, and lead. The material selection was limited due to the materials available in the GADRAS library. Therefore not all materials found in the composition of a building were available for the simulation. The thicknesses were of 5cm, 15cm, and 75cm, to reflect typical thicknesses of a door, inner wall, and outer enhanced wall respectively.

Subsequently, these simulated spectra are given as input to an identification algorithm based on an RBF-profile library, that was built at Purdue's Artificial Intelligence Systems Laboratory (AISL) described in reference [4].

## METHODOLOGY

In the work done in [4] there were simulated gamma-ray spectra with a 3x3 NaI detector, and built a library of 25 nuclides by using a radial basis function neural network (RBF) [5] for each nuclide, as shown in Figure 1.

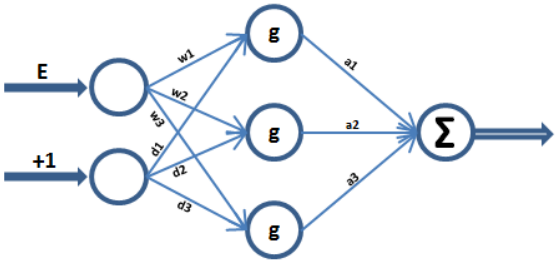


Fig. 1. Architecture of the RBF Neural Network, where $E$ is the input, $w_i$ and $a_i$ are the weights and g stands for the Gaussian activation function.

Each RBF is of the form

$$\phi(E,a,\mu,\sigma)=\sum_{i=1}^{M} a_i e^{-\frac{1}{2}\left(\frac{E-\mu_i}{\sigma_i}\right)^2} \quad (1)$$

where $w_i=\frac{1}{\sigma_i}, d_i=-\frac{\mu_i}{\sigma_i}$ while $g(x)=e^{-\frac{1}{2}x^2}$

and normalized so as $\int_0^\infty \phi(E,a,\mu,\sigma)dE=1$

Then, based on that library $(\phi_i \forall i=1,...,25)$ a method for identifying the presence of a nuclide in a given spectrum was developed. Let S(E) be the normalized spectrum such that

$$\int_0^\infty S(E)dE=1 \quad (2)$$

We assume that the spectrum can be written as a linear combination of the library functions as

$$S(E)=\sum_{i=1}^{25} p_i\phi_i(E) \quad (3)$$

$$\text{with } p_i\geq 0 \text{ and } \sum_{i=1}^{25} p_i=1 \quad (4)$$

The coefficients $p_i$ denote the relative contribution to counts due to the nuclide with profile $\phi_i(E)$ (count percentages) and are determined by minimizing the "error" function

$$\sum_{j=1}^{1024}(S(E_j)-\sum_{i=1}^{25}p_i\phi_i(E_j))^2 \qquad (5)$$

subject to constraints in (4). The error function was minimized using the BFGS method through the MERLIN optimization environment [6].

In this work, we aim to test the sensitivity of this algorithm to increasing levels of shielding. More specifically we tested the method for three different materials; concrete with density of 2.3 g/cm$^3$ ,atomic number AN=11.15 and areal density AD=2.7 g/cm$^3$ , lead with density of 11.35 g/cm$^3$, AN=82 and AD=2.7 g/cm$^3$ and wood of 0.54 g/cm$^3$, AN=6.14 and AD=2.7 g/cm$^3$. All three materials were tested for three different thicknesses of 5, 15 and 75 cm each. For this purpose, we have chosen nuclides which were included in that library; more specifically $^{60}$Co, $^{137}$Cs, $^{22}$Na, and $^{235}$U and simulated gamma-ray spectra with the pre-mentioned shielding.

## RESULTS

To obtain the simulated spectra we used GADRAS software [3].

Tables I through III list the results for each nuclide source used. The obtained percentages correspond to the relative contribution of each of the 25 nuclides included in the library, showing if they can be detected with a NaI detector. Note that only the nuclides showing 10% or more are listed due to an empirical threshold.

Table I shows the results when using $^{60}$Co for the source nuclide. As seen, $^{60}$Co is detected for all cases except lead with a thickness of 75 cm. This can be attributed to the thickness of the lead shielding. Lead is a strong shielding material and its effect is shown in Figs.2-4 where we can observe that as we increase the shielding level, the Cobalt peaks decrease.

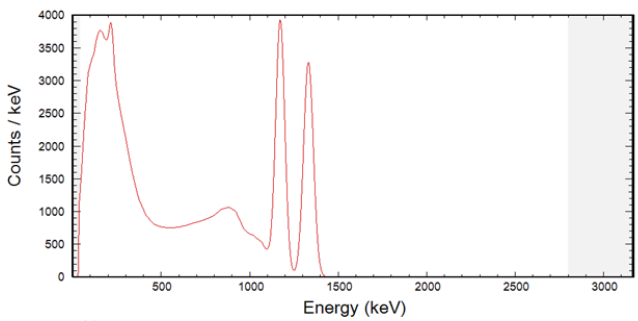


Fig. 2. $^{60}$Co spectrum with no shielding.

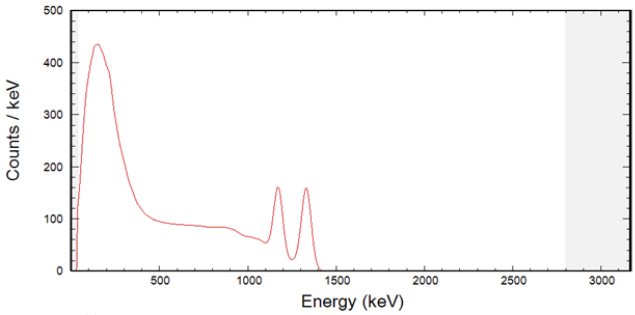


Fig. 3. $^{60}$Co spectrum with 5 cm lead shielding.

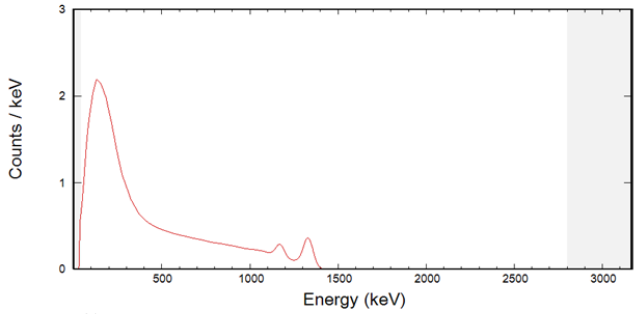


Fig. 4. $^{60}$Co spectrum with 15 cm lead shielding.

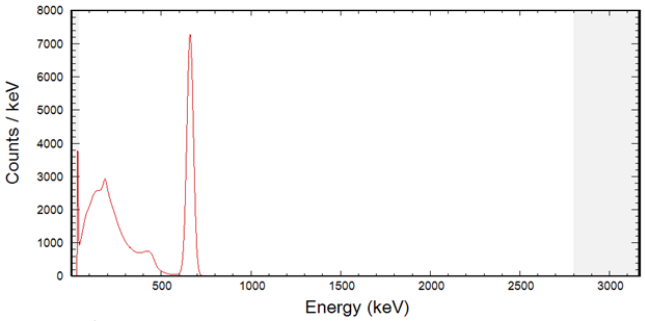


Fig. 5. $^{137}$Cs spectrum with no shielding.

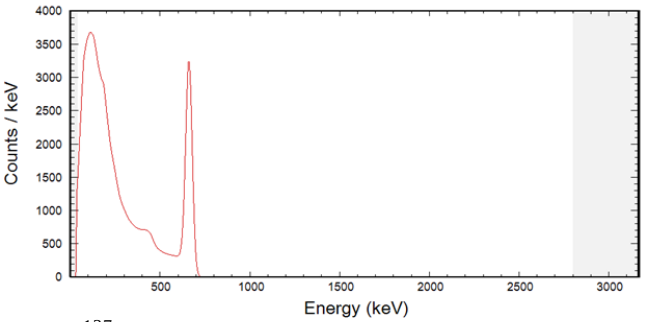


Fig. 6. $^{137}$Cs spectrum with 5 cm concrete shielding.

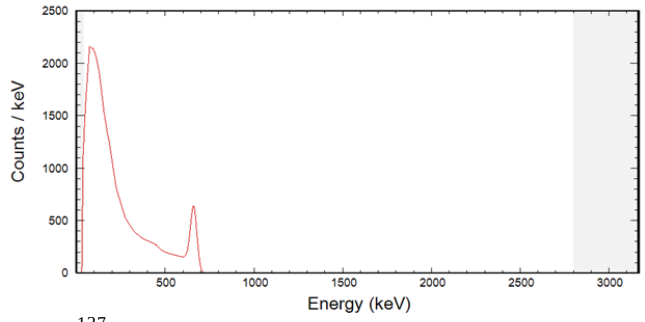


Fig. 7. $^{137}$Cs spectrum with 15 cm concrete shielding.

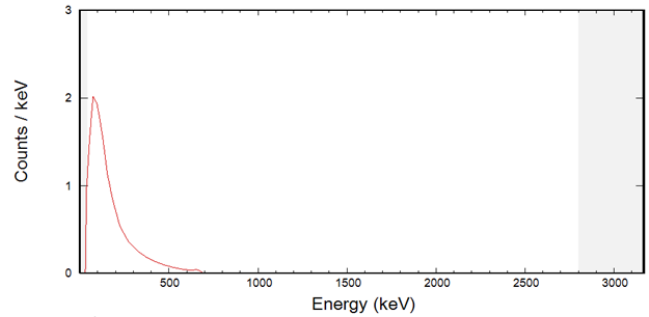


Fig. 8. $^{137}$Cs spectrum with 75 cm concrete shielding.

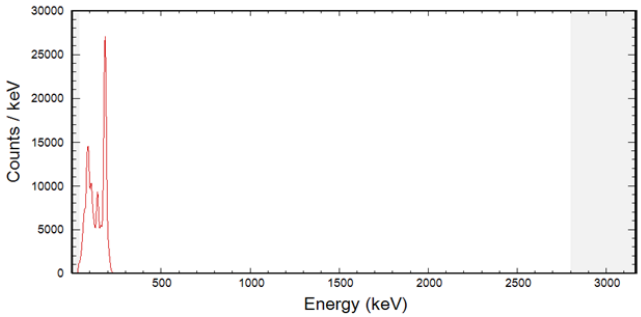


Fig. 9. $^{235}$U spectrum with no shielding.

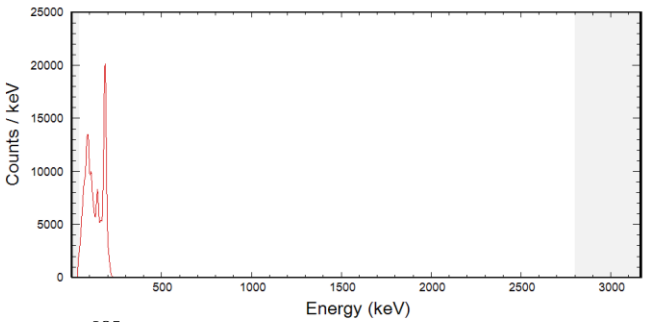


Fig. 10. $^{235}$U spectrum with 5 cm wood shielding.

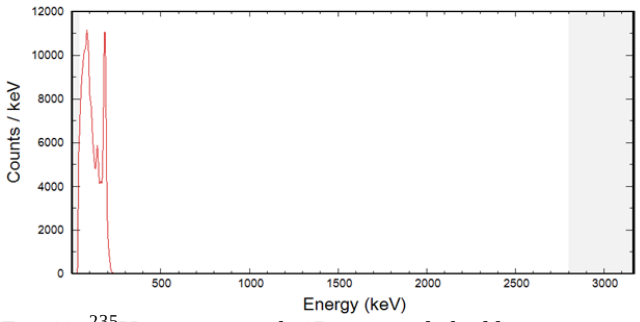


Fig. 11. $^{235}$U spectrum with 15 cm wood shielding.

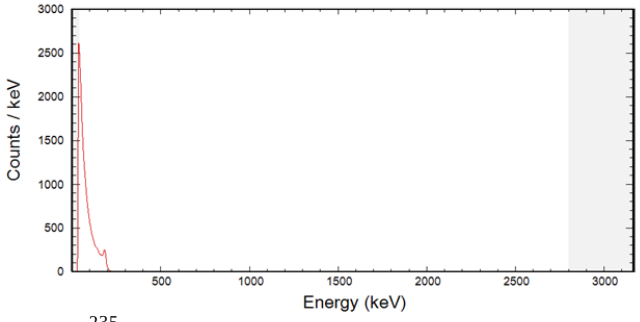


Fig. 12. $^{235}$U spectrum with 75 cm wood shielding.

TABLE I. Results for $^{60}$Co

| | Concrete | Lead | Wood |
|---|---|---|---|
| 5 cm | 46.1% $^{60}$Co, 10.4% $^{22}$Na | 45.6% $^{60}$Co, 14.2% $^{22}$Na, 13.2% $^{56}$Co | 70.5% $^{60}$Co, 15.1% $^{24}$Na |
| 15 cm | 25.4% $^{60}$Co | 32.3% $^{60}$Co, 13.4% $^{56}$Co, 11.3% $^{24}$Na, 11.5% $^{88}$Y | 53.1% $^{60}$Co, 11.8% $^{24}$Na |
| 75 cm | 8.8% $^{60}$Co, 14.4% $^{232}$U | | 20.9% $^{60}$Co, 10.4% $^{232}$U, 10.2% $^{133}$Ba |

Table II shows the results for $^{137}$Cs. Similar to the $^{60}$Co results, all cases show $^{137}$Cs as the main nuclide except for the case where concrete was used with a thickness of 75 cm. In this case, $^{133}$Ba is the nuclide with the largest percent. These results can be attributed to a few causes. First, as the shielding level is increased, the source will not be as easy to detect. This can be seen in Figs. 5 through 8. In these figures we observe the photopeak for $^{137}$Cs decreasing until it becomes indistinguishable (Fig. 12). Secondly, the reasoning for $^{133}$Ba being detected is because it has a similar photopeak as $^{137}$Cs; both nuclides have peaks around 81 keV.

TABLE II. Results for Cs137

| | Concrete | Lead | Wood |
|---|---|---|---|
| 5 cm | 47.3% $^{137}$Cs | 52.3% $^{137}$Cs | 80.8% $^{137}$Cs |
| 15 cm | 21.64% $^{137}$Cs, 13.57% $^{232}$U | | 56.4% $^{137}$Cs |
| 75 cm | 15.47% $^{133}$Ba, 2.42% $^{137}$Cs, 16.54% $^{232}$U, 10.5% $^{235}$U, 11% $^{237}$U | | 18% $^{137}$Cs, 15% $^{133}$Ba |

Table III shows the results for $^{22}$Na. A noticeable trend during this experiment was that over the lead shielding we did not get satisfying results but we noticed that the $^{22}$Na peak becomes less distinguishable and as we increase the shielding it disappears completely.

TABLE III. Results for $^{22}$Na

| | Concrete | Lead | Wood |
|---|---|---|---|
| 5 cm | 42% $^{22}$Na | 34.5% $^{60}$Co, 24.3 $^{56}$Co, 4.05% $^{22}$Na, 11.4% $^{88}$Y | 77.8% $^{22}$Na |
| 15 cm | 15.1% $^{22}$Na, 11.4% $^{232}$U | 19.4% $^{58}$Co, 19.4% $^{60}$Co, 15.1% $^{137}$Cs, 7.12% $^{22}$Na | 51.9% $^{22}$Na |
| 75 cm | 2.08% $^{22}$Na | | 14.6% $^{133}$Ba, 11.6% $^{22}$Na, 10.7% $^{232}$U |

In Table IV we can observe that the wood shielding was weak and allows us to detect the $^{235}$U. This can be observed in Figs. 9 through 12 which show the simulated $^{235}$U spectrum with no shielding, with 5 cm of wood shielding, with 15 cm of wood shielding, and with 75 cm of wood shielding. While under the lead shielding there was no $^{235}$U peak detected, since the $^{235}$U is difficult to detect with a NaI detector, due to lack of high resolution and we were unable to get any counts.

TABLE IV. Results for $^{235}$U

| | Concrete | Lead | Wood |
|---|---|---|---|
| 5 cm | 29.7% $^{235}$U, 16.2% $^{139}$Ce, 11.4% $^{166}$Ho | | 47.4% $^{235}$U, 15.7% $^{139}$Ce, 14.3% $^{232}$U |
| 15 cm | 13.4% $^{139}$Ce, 12.5% $^{235}$U, 12.2% $^{233}$U, 12.14% $^{133}$Ba, 10.3% $^{232}$U | | 28.8% $^{235}$U, 15.8% $^{139}$Ce, 13.2% $^{232}$U, 11.6% $^{166}$Ho |
| 75 cm | | | |

## CONCLUSION

We have tested the performance of the identification procedure described in [4], in the presence of a number of different shields made of concrete, lead and wood, i.e. materials commonly found in structural building blocks. We find that lead provides an effective shield, while concrete and wood let the gamma-rays pass through easier. Hence, the method will detect radioactive sources shielded with an average of 15cm, but will fail (as any other passive method) when the shield is such that it blocks, to great extent, the passage of gamma-rays. However, the existence of shields may be detected using different techniques, for instance by x-ray scanning. Hence a cargo may be considered suspicious if it is found to contain shielding materials.

## ACKNOWLEDGMENTS

The authors would like to acknowledge the Consortium for Nonproliferation Enabling Capabilities (CNEC) for funding this research.

## REFERENCES

1. J. MEDALIA, “Detection of nuclear weapons and materials: Science, technologies, observations”, *Congressional Research Service* 7-5700, R40154 (2010).
2. M. ALAMANIOTIS, A. HEIFETZ, A. C. RAPTIS, L. H. TSOUKALAS “Fuzzy-Logic Radioisotope Identifier for Gamma Spectroscopy in Source Search.” *IEEE Trans. on Nucl. Scien.*, **60**, 3014 (2013).
3. D. J. MITCHELL, “Gamma detector response and analysis software (GADRAS),” *Sandia National Laboratories, SAND88-2519* (1988).
4. P. L. LAGARI, “An RBF Neural Network Approach in Radionuclide Identification of Unknown Sources Utilizing γ-ray Spectra”, Master Thesis, Purdue University (2017).
5. L. H. TSOUKALAS, & R. E UHRIG, *Fuzzy and Neural Approaches in Engineering*, Wiley Interscience, New York, NY (1997).
6. D. G. PAPAGEORGIOU, I. N. DEMETROPOULOS, and I. E. LAGARIS, “Merlin-3.0 a multidimensional optimization environment,” Comp. Phys. Commun., **109**, 227 (1998).